Viral Dynamics of Primary Viremia and Antiretroviral Therapy in Simian Immunodeficiency Virus Infection

MARTIN A. NOWAK,[1] ALUN L. LLOYD,[1] GABRIELA M. VASQUEZ,[2] THERESA A. WILTROUT,[2]
LINDA M. WAHL,[1] NORBERT BISCHOFBERGER,[3] JON WILLIAMS,[4] AUDREY KINTER,[5]
ANTHONY S. FAUCI,[5] VANESSA M. HIRSCH,[6] AND JEFFREY D. LIFSON[2]*

*Mathematical Biology Group, Department of Zoology, University of Oxford, Oxford, England[1]; Laboratory of Retroviral
Pathogenesis, AIDS Vaccine Program, SAIC Frederick, National Cancer Institute-Frederick Cancer Research and
Development Center, Frederick, Maryland 21702[2]; Gilead Sciences, Inc., Foster City, California 94404[3]; Magainin
Pharmaceuticals, Inc., Plymouth Meeting, Pennsylvania 19462[4]; Laboratory of Immunoregulation, National Institute
of Allergy and Infectious Diseases, National Institutes of Health, Bethesda, Maryland 20852[5]; and
Laboratory of Infectious Diseases, National Institute of Allergy and Infectious Diseases,
National Institutes of Health, Rockville, Maryland 20892[6]*

Mathematical modeling of viral replication dynamics, based on sequential measurements of levels of virion-associated RNA in plasma during antiretroviral treatment, has led to fundamental new insights into human immunodeficiency virus type 1 pathogenesis. We took advantage of the simian immunodeficiency virus (SIV)-infected macaque model to perform detailed measurements and mathematical modeling during primary infection and during treatment of established infection with the antiretroviral drug (R)-9-(2-phosphonylmethoxypropyl)adenine (PMPA). The calculated clearance half-life for productively infected cells during resolution of the peak viremia of primary infection was on the order of 1 day, with slightly shorter clearance half-lives calculated during PMPA treatment. Viral reproduction rates upon discontinuation of PMPA treatment after 2 weeks were approximately twofold greater than those obtained just prior to initiation of treatment in the same animals, likely reflecting accumulation of susceptible target cells during treatment. The basic reproductive ratio (R_0) for the spread of SIV infection in vivo, which represents the number of productively infected cells derived from each productively infected cell at the beginning of infection, was also estimated. This parameter quantifies the extent to which antiviral therapy or vaccination must limit the initial spread of virus to prevent establishment of chronic disseminated infection. The results thus provide an important guide for efforts to develop vaccines against SIV and, by extension, human immunodeficiency virus.

Quantitative studies of viral replication in human immunodeficiency virus type 1 (HIV-1)-infected subjects have been enabled by sensitive new assay methods for measuring viral RNA in plasma (4, 20, 27, 28, 35). Results obtained with these techniques have led to revision of prevailing paradigms of AIDS pathogenesis, in part based on mathematical modeling of viral replication dynamics, facilitated by sequential plasma viral RNA measurements in patients responding to potent antiretroviral treatment regimens (2, 3, 5, 12, 17, 21–23, 25, 37). Modeling of the viral dynamics of primary HIV-1 infection has proved more difficult, due largely to the difficulties of obtaining specimens from the period immediately following infection.

The simian immunodeficiency virus (SIV)-infected macaque has been established as one of the preferred animal models for studies of AIDS virus pathogenesis, given the similarities between the genetic organization and in vivo pathogenesis of HIV-1 and SIV (14). With the recent development of sensitive techniques for quantification of plasma SIV RNA levels (8, 11, 16, 33, 36), studies with SIV-infected macaques have documented extensive ongoing viral replication throughout the course of infection, as well as correlations between different patterns of viral replication and clinical course, similar to those

demonstrated for HIV-1-infected patients (11, 18, 19, 24, 36). The ability to precisely control the inoculum used and the timing, amount, and route of inoculation, and to obtain multiple specimens early in infection at defined times following inoculation, makes the SIV-infected macaque model especially well suited for studies of primary infection.

We therefore utilized a sensitive quantitative competitive reverse transcription-PCR (QC-RT-PCR) assay for monitoring SIV RNA in longitudinal specimens and intensively characterized the viral dynamics of primary SIV infection in macaques to perform mathematical modeling of in vivo viral replication. The availability of (R)-9-(2-phosphonylmethoxypropyl)adenine (PMPA), a potent antiretroviral agent active against SIV (34), also allowed us to model the dynamics of treatment-associated decreases in viral replication and the rebound of viral replication when treatment was withdrawn. The results further reinforce the relevance and utility of the SIV-infected macaque as an animal model for HIV-1 infection of humans and provide insights into pathogenesis that would be difficult or impossible to obtain from studies of human subjects.

MATERIALS AND METHODS

Virus stocks. The isolation and characterization of SIVsmE660 and SIVsmE543-3 have been reported in detail elsewhere (7, 10). Infectious stocks of each virus were prepared by propagation in phytohemagglutinin A-activated peripheral blood mononuclear cells (PBMC) from *Macaca nemestrina*. Virus stocks were cryopreserved in vapor-phase liquid nitrogen until use.

Animal infections. All inoculations were by the intravenous route, to minimize potential between-animal differences due to differential transmission across mu-

* Corresponding author. Mailing address: Laboratory of Retroviral Pathogenesis, AIDS Vaccine Program, SAIC-Frederick, National Cancer Institute-Frederick Cancer Research and Development Center, Building 535, Room 509, Frederick, MD 21702. Phone: (301) 846-5019. Fax: (301) 846-5588. E-mail: lifson@avpvx1.ncifcrf.gov.

cosal barriers. For studies of primary SIV infection, 12 *M. nemestrina* animals (3 to 4 kg in body weight at the time of inoculation) received 50 50% monkey infectious doses of a cell-free stock of SIVsmE660 (7). One additional *M. nemestrina* macaque (PT 459; 4 kg at the time of inoculation) that had received 50 50% monkey infectious dose units (intravenous infectivity titration in *M. nemestrina*) of the same virus stock was used for studies of viral load response to PMPA treatment. For detailed studies of primary infection and PMPA treatment, two *Macaca mulatta* macaques (Rh-H352 and Rh-E911; 3 to 5 kg at the time of inoculation) received 1,000 50% tissue culture infectious doses (titers determined on phytohemagglutinin A-activated PBMC from *M. nemestrina*) of a cell-free stock of SIVsmE543-3 produced in phytohemagglutinin A-activated PBMC from *M. nemestrina*.

Specimens for plasma viral load. Plasma samples were obtained from acid citrate-dextrose-A anticoagulated whole blood. Specimens were processed within 3 h of phlebotomy, and cell-free plasma samples prepared by sequential centrifugation were cryopreserved at −70°C until analysis (11).

Primary SIVsmE660 infection. Plasma SIV RNA levels were measured by QC-RT-PCR twice weekly, through the first 6 weeks of infection, beginning on day 4 postinoculation (11).

Primary SIVsmE543-3 infection. Daily plasma viral RNA measurements were performed through the first 2 weeks postinoculation, with continued measurements through the first 5 weeks of follow-up.

PMPA treatment. PMPA was provided by Gilead Sciences, Inc. (Foster City, Calif.). After three baseline plasma viral load measurements were obtained, animals with established SIV infection received 30 mg of PMPA subcutaneously per kg of body weight, once daily for a period of 2 weeks, after which treatment was withdrawn, with continued intensive monitoring of plasma viral load levels through 2 additional weeks of follow-up.

Plasma viral load measurements. RNA was extracted from acid citrate-dextrose-A anticoagulated plasma specimens with commercial reagents (Puregene; Gentra Systems, Minneapolis, Minn.). QC-RT-PCR analysis was based on a highly conserved region of the SIV *gag* sequence (11). QC-RT-PCR of plasma virion-associated RNA was performed essentially as described in detail elsewhere by using purified, quantified in vitro transcripts of the internally deleted SIV *gag* control construct pSGΔ83, random-primed murine leukemia virus reverse transcriptase-catalyzed RT, and PCR amplification (45 cycles: 94°C, 60 s; 55°C, 120 s; 72°C, 60 s) of the resulting cDNA with the primers S-GAG03 (5′-CAGGGAAiiiAGCAGATGAATTAG-3′, where i indicates inosine) and S-GAG04 (5′-GTTTCACTTTCTCTTCTGCGTG-3′) (11). The products were quantified by computer-assisted video image analysis of ethidium bromide-stained gels. Interassay variation was <25% (coefficient of variation).

Mathematical modeling of primary infection. The primary phase of SIV infection was modeled by using the standard mathematical model of viral dynamics (2, 4–6, 9, 21–23, 25, 26, 32, 37). The model (depicted in Fig. 1) has three variables: uninfected cells, x; infected cells, y; and free virus particles, v. The model assumes that uninfected cells are produced at a constant rate, λ, and die at the rate dx. Free virus infects uninfected cells to produce infected cells at rate βxv. Infected cells die at rate ay. New virus is produced from infected cells at rate ky and decays (is cleared) at rate uv. The average lifetimes of uninfected cells, infected cells, and free virus are thus given by $1/d$, $1/a$, and $1/u$, respectively. The average number of virus particles produced over the lifetime of a single infected cell (the burst size) is given by k/a. These assumptions lead to the differential equations

$$\mathrm{d}x/\mathrm{d}t = \lambda - dx - \beta\,xv, \quad \mathrm{d}y/\mathrm{d}t = \beta\,xv - ay, \quad \text{and} \quad \mathrm{d}v/\mathrm{d}t = ky - uv.$$

Before infection ($y = 0$, $v = 0$), uninfected cells are at the equilibrium $x_0 = \lambda/d$. A small initial amount of virus, v_0, can propagate if its basic reproductive ratio, R_0, defined as the average number of newly infected cells that arise from any one productively infected cell when almost all cells are uninfected, is larger than one (1). Here $R_0 = \beta\lambda k/(adu)$. If $R_0 > 1$, then virus growth is initially exponential. The initial exponential growth rate, r_0, is given by the dominant root of the equation $r_0^2 + (a + u)r_0 + au(1 - R_0) = 0$. If u is much larger than a and r_0, then $r_0 = a(R_0 - 1)$. This can also be written as $r_0 = \beta' x_0 - a$ where $\beta' = \beta k/u$.

In the model, virus growth slows down as the supply of uninfected cells declines. Virus load reaches a maximum and then begins to decrease. Conversely, the abundance of uninfected cells reaches a minimum (designated by x_1) and then starts to increase again. The exponential rate of decline of virus load from its peak value is roughly given by $\alpha = a - \beta' x_1$. Therefore, the rate of virus decline from the primary peak represents a minimum estimate for the death rate of productively infected cells, a. Subsequently, the system converges in damped oscillations to the equilibrium specified by $x^* = (au)/(\beta k)$, $y^* = (R_0 - 1)$ $(du)/(\beta k)$, $v^* = (R_0 - 1)$ (d/β). At equilibrium, any one productively infected cell generates on average one new productively infected cell.

Mathematical modeling of antiretroviral treatment. Prior to treatment of established SIV infection, it can be assumed that free virus and infected and uninfected cells are at their equilibrium values, v^*, y^*, and x^*, respectively. This implies that $\beta' x^* = a$. For modeling purposes, it can be further assumed that during treatment the rate of new infection of uninfected cells, β, is reduced to zero. During treatment, virus load decreases and the abundance of uninfected target cells increases. When treatment is withdrawn, virus load increases in a roughly exponential manner with a rate given approximately by $r = \beta' x_2 - a$,
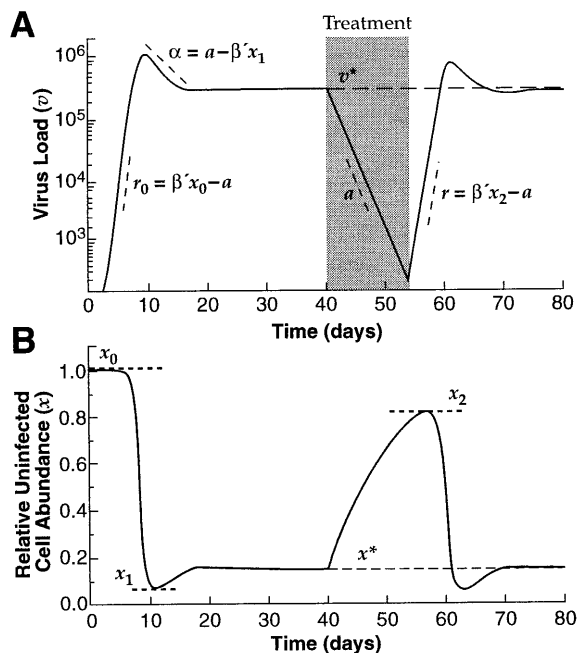

FIG. 1. Curves show computer-generated values obtained from the basic model of viral dynamics (see text) for plasma viral RNA (A) and relative uninfected cell abundance (B) through primary SIV infection, into the postacute phase of infection, and through the initiation and withdrawal of antiretroviral drug treatment. Parameters are as defined in the text. Absolute viral load values shown in panel A are representative values and are for purposes of illustration only.

where x_2 is the level of uninfected target cells at the time when treatment is withdrawn.

The parameter a is given by the decay slope of plasma virus during treatment while the parameter r is given by the slope of virus load increase once treatment is withdrawn. Therefore, comparisons can be made between the rate of production of newly infected cells per infected cell per day, before and after therapy, designated by $\beta' x^*$ and $\beta' x_2$, respectively.

Estimation of the basic reproductive ratio, R_0. From the standard model of viral dynamics, a relation between the basic reproductive ratio, R_0, and the initial exponential growth rate, r_0, can be derived: $R_0 = 1 + r_0 (r_0 + a + u)/au$. If $r_0 + a$ is small compared to u, then the relation approaches $R_0 = 1 + (r_0/a)$.

The standard model of virus dynamics, however, will underestimate the true basic reproductive ratio, if there is a significant time delay between infection of a cell and the time a cell starts to produce new virus particles. In more complicated models of virus dynamics that include such a time delay (9), the basic reproductive ratio is generally given by $R_0 = P\beta \lambda k/(adu)$, where P is the probability that an infected cell survives the delay time (15a). If this probability is close to one, then there is little difference in the expressions for R_0 values obtained by the standard model or by models accounting for this intracellular delay. In the absence of independent knowledge of all model parameters, R_0 can be estimated based on the relationship between the initial virus growth rate, r_0, and R_0. Inclusion of a delay, however, may have a significant impact on the relation between r_0 and R_0, since a delay in virus production leads to a reduction in the initial virus growth rate. For a model with a fixed time delay, τ, the relation can be expressed as $R_0 = (1 + r/a) \exp(r\tau)$. For a model with an exponentially distributed time delay (of mean value specified by τ), $R_0 = 1 + (r/a) [1 + (r + a)\tau]$. Both equations apply at the limit where u is much larger than a or r. The second equation also assumes that $1/\tau \gg d$.

RESULTS

Viral dynamics of primary SIV infection in *M. nemestrina*. Initial studies of longitudinal plasma specimens from 12 macaques that received identical inocula of SIVsmE660 demonstrated widely varying rates and levels of viral replication among animals (Fig. 2). At day 4 postinoculation, 4 of 12 animals had quantifiable levels of plasma viral RNA (>400 copy eq/ml) (Fig. 2 and Table 1). All 12 animals had quantifiable levels by day 7. Plasma viral RNA levels then rose to peak
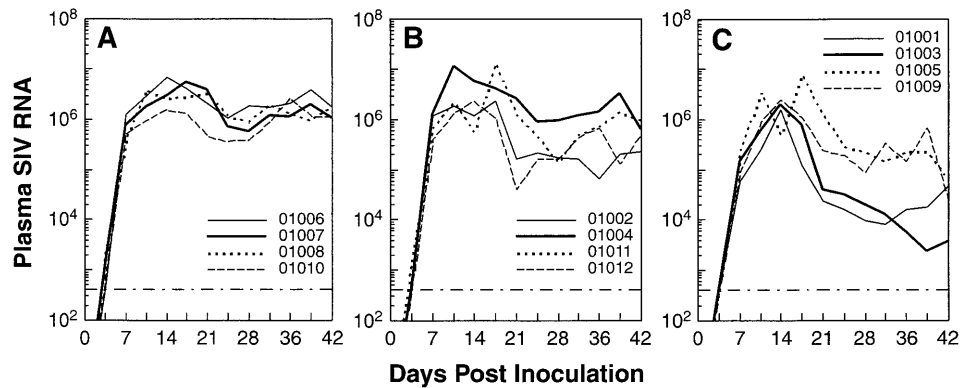
FIG. 2. Plasma viral load levels were monitored from inoculation through resolution of primary infection in 12 *M. nemestrina* macaques infected with SIVsmE660.

values over the succeeding 3 to 10 days and declined to quasi-steady-state levels in the postacute phase of infection, through day 42 postinoculation. Plasma virus levels in the postacute phase varied by nearly 3 logs among animals that had received identical inocula (compare, for example, animals 01003 and 01006 [Fig. 2A and C]). Plasma viral RNA levels measured on day 7 in these animals significantly predicted the postacute level that was established (15), underscoring the importance of differences in the rate and extent of very early viral replication in determining the prognostically significant postacute viral replication set point.

Detailed viral dynamics of primary SIV infection in *M. mulatta*. The dynamics of primary SIV infection were studied in greater detail for two rhesus macaques (*M. mulatta*) inoculated with a molecularly cloned SIV isolate, SIVsmE543-3 (10), to further minimize potential differences in viral replication attributable to viral factors. Daily plasma viral RNA measurements were performed through the first 2 weeks postinoculation, with continued measurements through the first 5 weeks of follow-up (Fig. 3). These data and the data shown in Fig. 2 were used for mathematical modeling of the viral dynamics of primary SIV infection (see below).

Viral dynamics of antiretroviral treatment with PMPA. To evaluate viral turnover in the setting of antiretroviral treatment, we used PMPA (34) as a means to block new rounds of viral replication. As in similar studies of treated HIV-1-infected patients (2, 3, 5, 6, 12, 22, 23, 25, 32, 37), this approach provides a maximum (upper limit) half-life for virus-producing cells, since it assumes that pharmacological blockade of new infection is both instantaneous and completely efficacious; actual values are likely somewhat lower. As shown in Fig. 4, viral load levels began to decrease within 2 days of initiation of treatment, decreasing within 2 weeks to nadir values 2 to 3 logs lower than pretreatment baselines. Upon withdrawal of treatment, plasma viral RNA levels rebounded to essentially pretreatment baseline levels within 2 weeks.

Mathematical modeling of primary SIV infection dynamics in *M. nemestrina*. Table 1 shows exponential virus growth rates for the 12 *M. nemestrina* animals as shown in Fig. 2, as estimated from virus load measurements at day 4 and day 7 postinoculation with SIVsmE660. Where plasma virus was below the threshold for quantification, the assay threshold limit, 400 copy eq/ml, was used for calculations. Thus, these values represent a minimum estimate. Exponential growth rates ranged

TABLE 1. Viral replication dynamic parameters in primary SIVsmE660 infection[a]

Animal no.	Plasma viral RNA (copy eq/ml)				Up slope		Down slope	
	day 4	day 7	Max (day of max)	days 36, 38, and 42	r	t_2	α	$t_{1/2}$
01001	400	58,000	1,600,000 (14)	27,000	1.66	0.42	0.86	0.80
01009	400	88,000	1,120,000 (17)	270,000	1.80	0.39	0.39	1.80
01003	400	144,000	800,000 (17)	3,900	1.96	0.35	0.35	0.93
01005	400	250,000	3,440,000 (10)	170,000	2.15	0.32	0.47	1.47
01012	400	400,000	1,040,000 (17)	440,000	2.30	0.30	0.82	0.85
01002	400	1,200,000	2,400,000 (17)	170,000	1.67	0.26	0.68	1.02
01008	2,400	400,000	3,200,000 (21)	1,400,000	1.71	0.41	0.33	2.12
01011	1,800	660,000	1,280,000 (17)	1,000,000	1.97	0.35	0.58	1.20
01007	1,200	740,000	3,840,000 (21)	1,400,000	2.14	0.32	0.57	1.23
01010	760	500,000	1,360,000 (17)	1,700,000	2.16	0.32	0.26	2.66
01004	400	1,300,000	2,640,000 (21)	1,800,000	2.69	0.26	0.37	1.89
01006	400	1,300,000	7,040,000 (14)	2,600,000	2.69	0.26	0.18	3.81
Geometric mean					2.20	0.32	0.52	1.33

[a] Twelve *M. nemestrina* animals were inoculated with SIVsmE660, and plasma was sampled twice weekly through day 42. The table shows viral load measurements on the indicated days that served as the basis of the calculations (days 4 and 7) and the day and value for peak primary plasma viremia (maximum [Max] and day of maximum). The postacute plasma viral RNA level was taken as the average of viral load measurements on days 36, 39, and 42 postinoculation. Parameters modeled include r, the per-day viral exponential growth rate; t_2, the plasma viral load doubling time, in days; α, the rate of decline of plasma virus from the peak value during primary infection; and $t_{1/2}$, the maximum (upper limit) decay half-life for free virus and productively infected cells, in days. r and t_2 are modeled from the slope from day 4 to day 7. α and $t_{1/2}$ are calculated from the steepest portion of the decay slope after the initial peak of plasma viral RNA. This value may be confounded by potentially changing rates of clearance of plasma virus during resolution of primary infection.
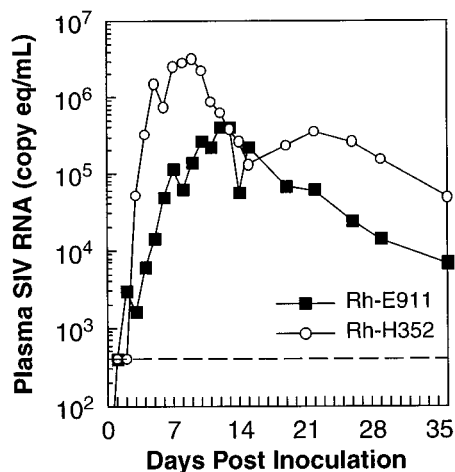
FIG. 3. Plasma viral load levels were monitored from inoculation through resolution of primary infection in two *M. mulatta* macaques infected with SIVsmE543-3.

from 1.7 to 2.7 per day, with an average of 2.2 per day, corresponding to doubling times of plasma virus levels ranging from 6 to 10 h. The decline of plasma virus from the peak value during primary infection (α) occurred with an average rate of 0.5 per day, equivalent to a half-life of 1.3 days. This provides a maximum (upper limit) clearance half-life for productively infected cells in SIV infection.

Mathematical modeling of viral clearance during PMPA treatment of SIV infection and comparison with clearance during resolution of primary infection. Frequent analyses of plasma viral RNA levels during PMPA administration (Fig. 4) provided the basis for mathematical modeling of antiretroviral drug treatment in SIV-infected macaques. PMPA is a reverse transcriptase inhibitor that blocks new rounds of SIV infection. The exponential decay slope of plasma viral RNA levels in treated animals thus reflects the turnover rate of productively infected cells present at the time of initiation of treatment. Clearance half-lives for these infected cells ranged from 0.7 to 1.4 days. Table 2 also includes calculated clearance half-lives for productively infected cells in animals Rh-H352 and Rh-E911 during primary infection and during PMPA treatment. This allowed a unique comparison of half-life ($t_{1/2}$) values calculated from the decay slope of plasma virus levels during resolution of the peak viremia of primary infection and the plasma virus decay slope seen upon initiation of PMPA treatment. Interestingly, this comparison revealed shorter clearance half-lives for infected cells during PMPA treatment.

Virus reproduction rates during different phases of infection. Experimentally, when PMPA treatment was withdrawn, plasma viral RNA levels rebounded. Plasma virus returned to approximately pretreatment levels but at slightly different rates in different animals. The calculated rates of virus production before and after treatment were compared (Table 2). Prior to treatment in the setting of established infection, uninfected cells, infected cells, and free virus are at roughly their equilibrium values of x^*, y^*, and v^*. Since $\beta' x^* = a$, in the quasiequilibrium state that obtains just prior to starting treatment, the rate of virus production, $\beta' x^*$, can be estimated as equivalent to the death rate of productively infected cells, a. The rate of virus production before treatment, $\beta' x^*$, can thus be compared to the rate of virus production when treatment is withdrawn, $\beta' x_2$. For Rh-E911, $\beta' x^* = 0.74$ and $\beta' x_2 = 1.5$. This suggests
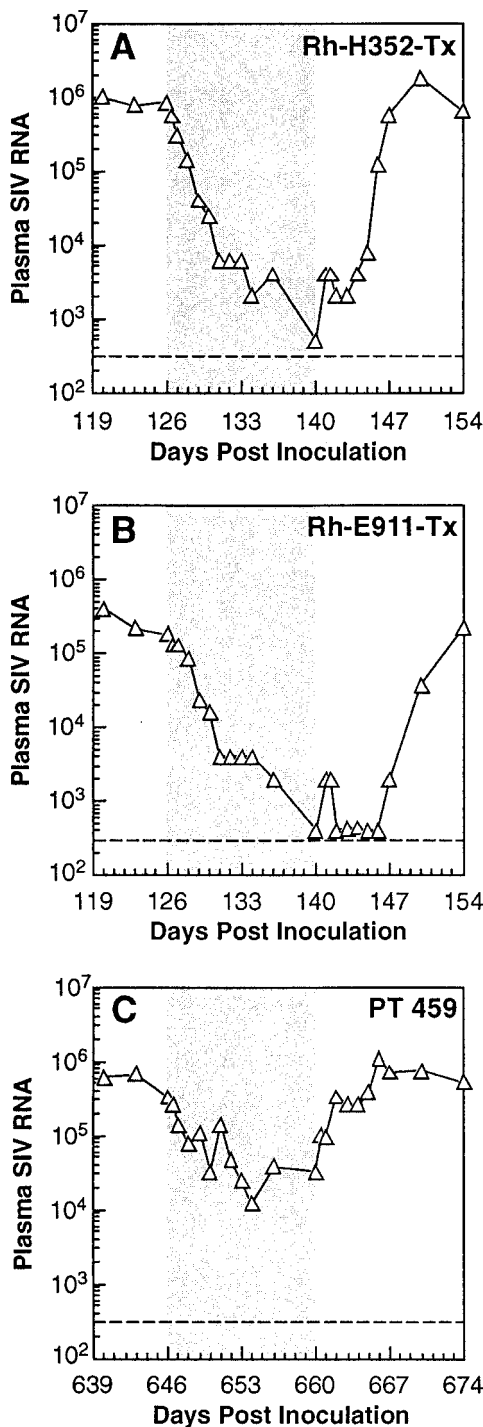

FIG. 4. Two *M. mulatta* macaques (Rh-H352 [A] and Rh-E911 [B]) macaques and one chronically SIV-infected *M. nemestrina* macaque (PT 459 [C]) macaque were treated with PMPA at the indicated times postinoculation. Shaded area indicates period of treatment. Results for primary infection for Rh-H352 and Rh-E911 are shown in Fig. 3; primary infection viral load data were not available for PT 459.

that target cell abundance (x) increased 2.4-fold in this animal during 2 weeks of treatment. Results for Rh-H352 and PT 459 ($\beta' x^* = 0.96$ and $\beta' x_2 = 2.40$ and $\beta' x^* = 0.51$ and $\beta' x_2 = 0.96$, respectively) imply 2.5-fold and 1.9-fold increases, respec-

TABLE 2. Viral replication dynamic parameters in primary SIVsmE543-3 infection and during initiation and cessation of PMPA treatment[a]

Animal	Primary infection parameter		PMPA treatment parameter		Calculated virus reproduction rate through the course of infection		
	r_0 (up slope)	α (down slope)	a (down slope)	r (up slope)	Day 0 (primary infection)	Pre-PMPA treatment (quasi-steady state)	End of PMPA treatment (off-treatment rebound)
Rh-H352	2.31 ± 0.38 (1–5)	0.53 ± 0.03 (9–15)	0.96 ± 0.04 (126–131)	1.47 ± 0.23 (146–154)	3.3	0.96	2.40
Rh-E911	0.88 ± 0.10 (1–7)	0.16 ± 0.04 (13–29)	0.74 ± 0.08 (126–131)	1.77 ± 0.13 (143–147)	1.6	0.74	1.50
PT 459			0.51 ± 0.10 (646–652)	0.45 ± 0.09 (660–668)		0.51	0.96

[a] Two *M. mulatta* macaques were inoculated with SIVsmE543-3, and plasma was sampled daily through 2 weeks and then twice weekly or weekly through day 35. Plasma virus levels were also measured through the course of initiation and withdrawal of PMPA treatment in these animals and one *M. nemestrina* macaque. Values shown, with standard errors, were calculated by linear regression analysis for the four to eight points covering the period of maximum slope for each interval (in days), indicated in parentheses after each value. Virus reproduction rates were calculated over the course of infection, from the initial exponential expansion of virus (day 0), just prior to the start of PMPA treatment (day 126, Rh-H352 and Rh-E911; day 646, PT 459), and after withdrawal of PMPA treatment (day 140, Rh-H352 and Rh-E911; day 660, PT 459). Viral dynamic parameters were calculated as described in the text.

tively, in target cell abundance. The alternative, less likely interpretation would be that the efficiency of viral transmission (β') increases twofold during treatment, for example, because of a decrease in antiviral immunity.

For animals Rh-E911 and Rh-H352, the rate of virus reproduction after withdrawal of treatment (r) can also be compared to the rate of virus reproduction during the exponential phase of viral replication in primary infection (r_0). For Rh-E911, $r_0 = 0.88$ per day and $r = 0.77$ per day. For Rh-H352, $r_0 = 2.31$ per day and $r = 1.47$ per day. Thus, in both animals the net rebound virus growth rate when treatment is withdrawn is slightly lower than the net virus growth rate during primary infection.

Basic reproductive ratio, R_0. The data also provide information on the basic reproductive ratio, R_0, for SIV replication in vivo. In the standard model, R_0 can be obtained from the exponential growth rate, r_0, during primary infection, and the death rate, a, of infected cells as $R_0 = 1 + r_0/a$. The experimentally determined values for r_0 range from 0.9 to 2.7 per day, with an average of 2.2 per day (Tables 1 and 2). Results obtained during PMPA treatment provide estimates for a ranging from 0.51 to 0.96, with an average value of 0.74. Taking the average value of $a = 0.74$, the variation in r_0 leads to calculated basic reproductive ratios, R_0, ranging from 2.2 to 4.6. This implies that, at the beginning of infection, when uninfected target cells predominate, each productively infected cell produces during its lifetime on average only two to five new productively infected cells.

However, the standard model of virus dynamics underestimates R_0 because it does not account for the time delay between infection of a cell and production of progeny virions. Incorporation of terms reflecting such intracellular delays increases the estimate of R_0 based on observations of the exponential growth rate, r_0. Calculations based on an exponentially distributed time delay of 24 h (9), on average, yield R_0 values ranging from 4.2 to 17 (Table 3). Inclusion of a fixed time delay (delta distribution) of 24 h leads to R_0 values ranging from 5.4 to 68 (Table 3). A model with a fixed time delay provides the highest possible estimate for R_0 while a model with an exponentially distributed delay provides the lowest estimate, for given values of a, r_0, and the average length of the time delay. Shorter time delays yield lower values of R_0. For example, calculations from our data with a model with a fixed time delay of 12 h (instead of the 24 h assumed in the calculations above) provide estimates of R_0 ranging from 3.5 to 10.

DISCUSSION

We took advantage of the ability to control virologic variables, and to obtain frequent early specimens at defined intervals from the known time of inoculation, to model the dynamics of viral replication in primary SIV infection of macaques, in a way that would not be possible in HIV-1-infected human subjects. These studies also allowed comparison of viral dynamic parameters determined during primary infection and during antiretroviral drug treatment of established infection in the same animals. While this analysis focused on the productively infected cell compartment that turns over rapidly, recent analyses of HIV-1-infected humans suggest that chronically infected cells such as macrophages and activation of latently infected cells contribute only minimally in quantitative terms to the circulating plasma virus pool (12, 25, 37).

The doubling time for plasma virus levels during the exponential phase of primary infection was calculated (t_2 [Table 1]), demonstrating that circulating virus levels double approximately every 6 to 10 h during this phase. This information, which would be very difficult to obtain from studies of human subjects, is of interest in understanding the contribution of early viral replication and spread in helping to determine the prognostically important postacute viral replication set point (11, 15, 18, 19, 24, 36). The values obtained for clearance half-lives during the resolution of primary infection (α [Table 1]) showed a relatively narrow range of variation among the animals studied, with an average value of 1.3 days that is comparable to calculations of infected cell clearance half-lives derived from studies of HIV-1-infected human subjects treated

TABLE 3. Calculated R_0 values during primary SIV infection[a]

Observed exponential growth rate during primary infection (r_0)	Calculated R_0 value		
	Standard model (no delay)	Exponentially distributed delay	Fixed delay
0.9	2.2	4.2	5.4
2.2	4.0	13	36
2.7	4.6	17	68

[a] Calculated values for the basic reproductive ratio, R_0, during primary SIV infection, either based on the standard model of viral dynamics (assuming no intracellular delay between infection and production of progeny virions) or assuming a delay that is exponentially distributed, with an average value of 1 day, or fixed at 1 day ($\tau = 1$). Results are shown for calculations with the average value for a ($a = 0.74$).

with antiretroviral drug regimens (2, 3, 5, 6, 12, 17, 21–23, 25, 32, 37).

In addition to analysis of viral replication in primary infection, measurements were also performed during established infection, both during the quasi-steady state that obtained just prior to treatment and during the periods of dynamic changes in viral replication associated with initiation and discontinuation of PMPA treatment. Measurements of plasma virus levels in animals in whom PMPA treatment was initiated and then withdrawn allowed comparison of the viral dynamics during resolution of primary infection and during drug treatment. Comparisons were also made of viral replication during primary infection and during established infection. The infected cell clearance half-lives determined during PMPA treatment were shorter than those measured during resolution of primary infection, including determinations in the same animals. As both values represent estimated upper limits, the lower upper limit values obtained during PMPA treatment more likely reflect the true infected cell clearance half-life. This may be explained by greater efficacy of blockade of new rounds of infection by PMPA compared to whatever mechanisms are responsible for limiting viral spread during resolution of primary infection. In addition, the mechanisms contributing to clearance of infected cells may have been operating more effectively during the period when the PMPA treatment data were obtained than during the period of decline from peak primary viremia levels.

The viral dynamics of withdrawal of antiretroviral drug treatment were also analyzed. During PMPA treatment, the abundance of SIV-susceptible but uninfected target cells is presumed to increase as infection of these cells is blocked by the drug and the cells are neither killed by lytic viral infection nor cleared by host immune mechanisms dependent on productive infection. Plasma virus levels decline, reflecting clearance of existing free virus and productively infected cells. However, when treatment is withdrawn, new infection of uninfected cells is no longer inhibited and viral replication and spread resume. According to the model, plasma viral load rises at first exponentially, with a growth rate given by $r = \beta' x_2 - a$, where x_2 designates the abundance of uninfected cells at the time when treatment is withdrawn (Fig. 1B). Comparison of calculated virus reproduction rates just before initiation of PMPA treatment and after discontinuation of treatment showed approximately twofold higher levels following discontinuation of treatment, consistent with such an increase in the availability of susceptible target cells during the period of treatment (Table 2).

For two animals, we compared the rate of virus reproduction upon withdrawal of PMPA treatment with the rate during the exponential phase of primary infection. In both macaques, the rate was slightly lower upon withdrawal of PMPA treatment than during the exponential phase of primary infection. This may reflect reduced levels of target cells during the period of drug withdrawal compared to initial infection and/or the effects of antiviral immunity that developed through the course of infection.

Our data also allowed calculation of the basic reproductive ratio (R_0) for primary SIV infection. By the standard model of viral dynamics, the values obtained for this parameter ranged between 2 and 5 in different animals. The standard model, however, does not account for the effects of any time delay between infection of a cell and production of progeny virions. With models that include such a delay and estimate R_0 based on the relationship between the initial growth rate r_0 and R_0 (9), the estimates of R_0 may increase. Estimates of R_0 based on a fixed time delay of 12 h range from 3.5 to 10 (Table 3). For
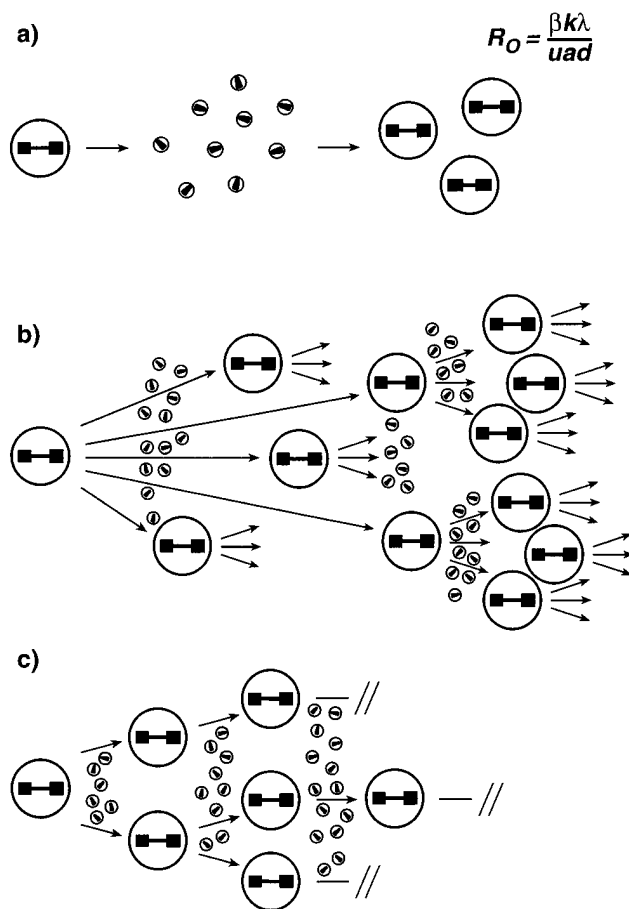

FIG. 5. Schematic diagram shows the viral basic reproductive ratio R_0 (a), including those for the cases in which sufficient early spread to establish a disseminated chronic infection either is ($R_0 > 1$) (b) or is not ($R_0 < 1$) (c) achieved.

a fixed time delay of 24 h, the estimates increase to a value from 5.4 to 68. Although the actual duration of this intracellular lag time in vivo is not known, it is unlikely to exceed 24 h for productively infected cells (13, 25). Moreover, if the delay time is not fixed but follows an exponential or gamma distribution around the same average length, then the estimates for R_0 will be reduced. Therefore, estimates based on a fixed 24-h delay can be considered a worst-case scenario.

The value of R_0 is extremely important for evaluating the possible success of vaccination or very early treatment. A vaccine that reduces the replication rate of the virus by a factor of R_0-fold should in principle prevent establishment of disseminated infection. Thus, with an R_0 value of 5, a vaccine regimen or postinoculation treatment that reduced initial viral replication rates by a factor approaching fivefold would result in less than one newly infected cell being produced from each infected cell. Such a reproduction rate is, of course, not compatible with maintenance of a spreading infection and should preclude establishment of a chronic disseminated systemic infection. Assuming R_0 remains at <1.0, the infection should eventually burn out as the initial infected cell population dies off (Fig. 5).

Even allowing for intracellular delays as noted above, the calculated values for R_0 are relatively low. Therefore, even comparatively modest perturbations due to immunological or

pharmacological influences, if they are operative at the point where they may prevent rapid dissemination of virus, may exert a significant impact on the establishment of infection. This may explain studies suggesting that prior immunological sensitization or postexposure treatment with antiretroviral agents may effectively prevent establishment of chronic systemic infection in both HIV and SIV systems (29–31, 34). Indeed, the fact that empirical data indicate that blockade of establishment of systemic SIV infection is indeed feasible with postinoculation treatment using currently available antiretroviral agents (34) implies that biologically significant intracellular delays and R_0 values are likely in the range suggested. Based on the modeling considerations outlined above, vaccine or early treatment regimens leading to approximately 2-log or greater decreases in early viral spread rates relative to untreated subjects should have an excellent chance of blocking establishment of disseminated chronic infection or dramatically modulating viral replication set points and associated clinical courses (11, 15). Additional refinement of this estimate of R_0 may provide further important insights into AIDS pathogenesis with ramifications for both treatment and vaccine-induced prevention of the establishment of infection.

The animals studied differed substantially in the initial growth rate for plasma viral load, with r_0 values ranging from 0.9 to 2.7 per day. Studies of the in vitro susceptibility to SIV infection of PBMC from the animals suggest that at least part of this difference may be related to differences in the intrinsic permissiveness for viral replication of target cells from different animals (15). We have also shown that the early in vivo virus growth rate is strongly correlated with the rate of disease progression (15). Therefore, the initial variation in virus growth rates is not simply measurement noise but does indeed reflect biologically important parameters. Since the value for r_0 determines our estimate for R_0, it is evident that animals with a low r_0 also have a low R_0. Even with the worst-case assumption of a fixed intracellular delay of 24 h, an r_0 of 0.9 per day corresponds to an R_0 of only 5.4. This implies that, in some animals (and by extension, in some humans), even rather inefficient vaccines may protect against establishment of chronic disseminated infection or may modulate the pattern of viral replication sufficiently to beneficially influence disease course (11, 15, 36).

Modulation of early viral replication may impact the subsequent viral replication set point that is established, in part through affecting the conditions and antigen load under which the initial antiviral immune response develops (15). Indeed, the fact that the range of plasma virus levels in the postacute phase of infection is broader than would be predicted by the basic mathematical model (9) but is still closely correlated with plasma virus levels measured on day 7 postinoculation (15) points to factors not included in the basic model, such as differences in host immune responses, influencing the postacute viral replication set point, in a manner that is in turn impacted by early viral replication levels.

In the aggregate, these observations and others arising from detailed monitoring of viral replication in SIV-infected macaques (11, 15, 36) emphasize the dynamic nature of retroviral replication, the critical importance of the period of initial infection in determining outcome, and the importance of differences between animals in determining differences in viral replication patterns and associated clinical course. The studies also further substantiate the importance of the SIV-infected macaque as a relevant animal model for HIV-1 infection and AIDS in humans. Additional studies of this type, in conjunction with detailed evaluation of the development of specific antiviral immune responses, should further clarify the viral and host factors involved in establishment of the viral replication set point in the postacute phase of infection. Finally, our estimates of the viral basic reproductive ratio, R_0, during primary SIV infection represent, to our knowledge, the first time this parameter has been calculated for an in vivo infection. The values obtained provide an estimate of the degree to which a vaccine will be required to block the initial burst of virus replication during primary infection if it is to prevent establishment of chronic disseminated infection or markedly delay disease progression, in the absence of true sterilizing immunity.

REFERENCES

1. **Anderson, R. M., and R. M. May.** 1991. Infectious diseases of humans. Oxford University Press, Oxford, United Kingdom.
2. **Bonhoeffer, S., J. Coffin, and M. A. Nowak.** 1997. Virus load and drug treatment. J. Virol. **71:**3275–3278.
3. **Bonhoeffer, S., R. M. May, G. M. Shaw, and M. A. Nowak.** 1997. Virus dynamics and drug treatment. Proc. Natl. Acad. Sci. USA **94:**6971–6976.
4. **Cao, Y., D. D. Ho, J. Todd, R. Kokka, M. Urdea, J. D. Lifson, M. Piatak, S. Chen, B. H. Hahn, M. S. Saag, and G. M. Shaw.** 1995. Clinical evaluation of branched DNA (bDNA) signal amplification for quantifying HIV-1 in human plasma. AIDS Res. Hum. Retroviruses **11:**353–361.
5. **Coffin, J. M.** 1995. HIV population dynamics in vivo: implications for genetic variation, pathogenesis and therapy. Science **267:**483–489.
6. **De Boer, R. J., and C. A. Boucher.** 1996. Anti-CD4 therapy for AIDS suggested by mathematical models. Proc. R. Soc. Lond. B Biol. Sci. **263:**899–905.
7. **Goldstein, S., W. R. Elkins, W. T. London, A. Hahn, R. Goeken, J. E. Martin, and V. M. Hirsch.** 1994. Immunization with whole inactivated vaccine protects from infection by SIV grown in human but not macaque cells. J. Med. Primatol. **23:**75–82.
8. **Grant, R. M., M. Kaur, H. A. McClure, A. Rosenthal, C. S. Horton, P. Carroll, R. P. Johnson, M. B. Feinberg, and S. I. Staprans.** 1996. Plasma SIV dynamics during primary viremia, abstr. 46. *In* 14th Annual Symposium on Nonhuman Primate Models for AIDS, 23 to 26 October 1996, Portland, Oreg.
9. **Herz, A. V., S. Bonhoeffer, R. M. Anderson, R. M. May, and M. A. Nowak.** 1996. Viral dynamics in vivo: limitations on estimates of intracellular delay and virus decay. Proc. Natl. Acad. Sci. USA **93:**7247–7251.
10. **Hirsch, V., D. Adger-Johnson, B. Campbell, S. Goldstein, C. Brown, W. R. Elkins, and D. C. Montefiori.** 1997. A molecularly cloned, pathogenic, neutralization-resistant simian immunodeficiency virus, SIVsmE543-3. J. Virol. **71:**1608–1620.
11. **Hirsch, V. M., T. R. Fuerst, G. Sutter, M. W. Carroll, L. C. Yang, S. Goldstein, M. Piatak, W. R. Elkins, D. C. Montefiori, B. Moss, and J. D. Lifson.** 1996. Patterns of viral replication correlate with outcome in simian immunodeficiency virus (SIV)-infected macaques: effect of prior immunization with a trivalent SIV vaccine in modified vaccinia virus Ankara. J. Virol. **70:**3741–3752.
12. **Ho, D. D., A. U. Neumann, A. S. Perelson, W. Chen, J. M. Leonard, and M. Markowitz.** 1995. Rapid turnover of plasma virions and CD4 lymphocytes in HIV-1 infection. Nature **373:**123–126.
13. **Klotman, M. E., S. Y. Kim, A. Buchbinder, A. DeRossi, D. Baltimore, and F. Wong-Staal.** 1991. Kinetics of expression of multiply spliced RNA in early human immunodeficiency virus infection of lymphocytes and monocytes. Proc. Natl. Acad. Sci. USA **88:**5011–5015.
14. **Letvin, N., and N. King.** 1990. Immunologic and pathologic manifestations of the infection of rhesus monkeys with simian immunodeficiency virus of macaques. J. Acquired Immune Defic. Syndr. **3:**1023–1040.
15. **Lifson, J. D., M. Nowak, S. Goldstein, J. L. Rossio, A. Kinter, G. Vasquez, T. A. Wiltrout, C. Brown, D. Schneider, L. Wahl, A. Lloyd, W. R. Elkins, A. S. Fauci, and V. M. Hirsch.** The extent of early viral replication is a critical determinant of the natural history of AIDS virus infection. Submitted for publication.
15a. **Lloyd, A. L., et al.** Unpublished data.
16. **Marx, P. A., A. I. Spira, A. Gettie, P. J. Dailey, R. S. Veazey, A. A. Lackner, C. J. Mahoney, C. J. Miller, L. E. Claypool, D. D. Ho, and N. J. Alexander.** 1996, Progesterone implants enhance SIV vaginal transmission and early virus load. Nat. Med. **2:**1084–1089.

17. **McLean, A. R., and M. A. Nowak.** 1992. Competition between zidovudine sensitive and resistant strains of HIV. AIDS **6:**71–79.
18. **Mellors, J. W., L. A. Kingsley, C. R. Rinaldo, Jr., J. A. Todd, B. S. Hoo, R. P. Kokka, and P. Gupta.** 1995. Quantitation of HIV-1 RNA in plasma predicts outcome after seroconversion. Ann. Intern. Med. **8:**573–579.
19. **Mellors, J. W., C. R. Rinaldo, Jr., P. Gupta, R. M. White, J. A. Todd, and L. A. Kingsley.** 1996. Prognosis in HIV-1 infection predicted by the quantity of virus in plasma. Science **272:**1167–1170.
20. **Mulder, J., N. McKinney, C. Christopherson, J. Sninsky, L. Greenfield, and S. Kwok.** 1994. Rapid and simple PCR assay for quantitation of human immunodeficiency virus type 1 RNA in plasma: application to acute retroviral infection. J. Clin. Microbiol. **32:**292–300.
21. **Nowak, M. A., and C. R. M. Bangham.** 1996. Population dynamics of immune responses to persistent viruses. Science **272:**74–79.
22. **Nowak, M. A., S. Bonhoeffer, C. Loveday, P. Balfe, M. Semple, S. Kaye, M. Tennant-Flowers, and R. Tedder.** 1995. HIV-1 dynamics: results confirmed. Nature **375:**193.
23. **Nowak, M. A., S. Bonhoeffer, G. M. Shaw, and R. M. May.** 1997. Antiviral drug treatment: dynamics of resistance in free virus and infected cell populations. J. Theor. Biol. **184:**203–217.
24. **O'Brien, T., W. A. Blattner, D. Waters, E. Eyster, M. W. Hilgartner, A. R. Cohen, N. Luban, A. Hatzakis, L. M. Aledort, P. S. Rosenberg, W. J. Miley, B. L. Kroner, J. J. Goedert, et al.** 1996. Serum HIV-1 RNA levels and time to development of AIDS in the multicenter hemophilia cohort study. JAMA **276:**105–110.
25. **Perelson, A. S., A. U. Neumann, M. Markowitz, J. M. Leonard, and D. D. Ho.** 1996. HIV-1 dynamics in vivo: virion clearance rate, infected cell life span, and viral generation time. Science **271:**1582–1586.
26. **Phillips, A. N.** 1996. Reduction of HIV concentration during acute infection: independence from a specific immune response. Science **271:**497–499.
27. **Piatak, M., K.-C. Luk, B. Williams, and J. D. Lifson.** 1993. Quantitative competitive polymerase chain reaction (QC-PCR) for accurate quantitation of HIV DNA and RNA species. BioTechniques **14:**70–77.
28. **Piatak, M., M. S. Saag, L. C. Yang, S. J. Clark, J. C. Kappes, K.-C. Luk, B. H. Hahn, G. M. Shaw, and J. D. Lifson.** 1993. High levels of HIV-1 in plasma during all stages of infection determined by competitive PCR. Science **259:**1749–1754.
29. **Rowland-Jones, S., J. Sutton, K. Ariyoshi, T. Dong, F. Gotch, S. McAdam, D. Whitby, S. Sabally, A. Gallimore, and T. Corrah.** 1995. HIV-specific cytotoxic T-cells in HIV-exposed but uninfected Gambian women. Nat. Med. **1:**59–64.
30. **Rowland-Jones, S. L., and A. McMichael.** 1995. Immune responses in HIV-exposed seronegatives: have they repelled the virus? Opin. Immunol. **7:**448–455.
31. **Shearer, G. M., and M. Clerici.** 1996. Protective immunity against HIV infection: has nature done the experiment for us? Immunol. Today **17:**21–24.
32. **Stilianakis, N. I., C. A. Boucher, M. D. De Jong, R. Van Leeuwen, R. Schuurman, and R. J. DeBoer.** 1997. Clinical data sets of human immunodeficiency virus type 1 reverse transcriptase-resistant mutants explained by a mathematical model. J. Virol. **71:**161–168.
33. **Travis, B. M., A. Watson, J. Ranchalis, N. L. Haigwood, and S. L. Hu.** 1996. Comparative QC-PCR analysis of viral load in macaques infected by primate lentiviruses: plasma SIV dynamics during primary viremia, abstr. 119. *In* 13th Annual Symposium on Nonhuman Primate Models for AIDS, 5 to 8 November 1996, Monterey, Calif.
34. **Tsai, C.-C., K. E. Follis, A. Sabo, T. W. Beck, R. F. Grant, N. Bischofberger, R. E. Benveniste, and R. Black.** 1995. Prevention of SIV infection by R-9-(2-phosphonylmethoxyproply)adenine et al. Science **270:**1197–1199.
35. **Van Gemen, B., P. van der Wiel, R. van Beuningen, P. Sillekens, S. Jurriaans, C. Dries, R. Schoones, and T. Kievits.** 1995. The one tube quantitative HIV-1 RNA NASBA: precision, accuracy, and application. PCR Methods Appl. **4:**S177–S184.
36. **Watson, A., J. Ranchalis, B. Travis, J. McClure, W. Sutton, P. R. Johnson, S.-L. Hu, and N. L. Haigwood.** 1997. Plasma viremia in macaques infected with simian immunodeficiency virus: plasma viral load early in infection predicts survival. J. Virol. **71:**284–290.
37. **Wei, X., S. K. Ghosh, M. E. Taylor, V. A. Johnson, E. A. Emini, P. Deutsch, J. D. Lifson, S. Bonhoeffer, M. A. Nowak, B. H. Hahn, M. S. Saag, and G. M. Shaw.** 1995. Viral dynamics in human immunodeficiency virus type 1 infection. Nature **373:**117–122.